Abde Imadjid Atassi[1], Mounir Djellab[1,2], Hamza Bentrah[1,2], Abdelouahad Chala[1], Mohamed Cherif Ben Ameur[3],Slimane Kherief[1], Ridha Azzouz[1,4], Amir Eddine Kabouia[1], Bouzid Bouamra[1]*

[1]Laboratory of Physics of Thin Films and Applications, University of Biskra, B.P. 145, Biskra, R.P. 07000 Algeria, [2]Laboratoire de Génie des procédés chimiques et de l'environnement, University of Biskra, B.P. 145, Biskra, R.P. 07000 Algeria, [3]Politecnico di Milano, Department of Chemistry, Materials and Chemical Engineering "Giulio Natta", Via Mancinelli, 7, 20131 Milano MI, Italy, [4]Centre de recherche scientifique et technique des régions arides de Biskra, University of Biskra, B.P. 145, Biskra, R.P. 07000 Algeria.

Scientific paper
ISSN 0351-9465, E-ISSN 2466-2585
https://doi.org/10.62638/ZasMat1393

Zastita Materijala 66 ( )
(2025)

Corrosion inhibition efficiency of the Myrrh Gum on API 5CTP110 tubing in hydrochloric acid

ABSTRACT

The corrosion inhibition properties of Myrrh Gum (MG) on API 5CTP110 tubing in a 0.5 M HCl solution were investigated using electrochemical techniques, including electrochemical impedance spectroscopy and potentiodynamic polarization. The study demonstrated that MG exhibits exceptional inhibitory performance, achieving an efficiency of 92% at an optimal concentration of 3 g/L. The analysis revealed that the adsorption of MG molecules onto the steel surface follows the Langmuir isotherm model, indicating a process dominated by physical adsorption. Additionally, MG acts as a mixed-type inhibitor, effectively mitigating both anodic and cathodic reactions. These findings highlight the potential of Myrrh Gum as a cost-effective and environmentally friendly corrosion inhibitor for industrial applications, particularly in acidic environments. The use of MG aligns with sustainable practices, providing a viable alternative to traditional synthetic inhibitors and contributing to the development of green corrosion prevention strategies.

***Keywords**: Eco-friendly corrosion inhibitor, API 5CTP110 tubing, Myrrh Gum,Hydrochloric acid,EIS*

1. INTRODUCTION

Carbon steels play a pivotal role in the petroleum industry, serving as the primary material for constructing vital oil and gas pipelines that facilitate exploration, extraction, and transportation processes within petroleum fields [1, 2]. Despite their widespread use driven by economic factors, carbon steel pipelines may encounter corrosion resistance challenges compared to alternative steel types [3]. While carbon steel is cost-effective and boasts properties essential for industrial applications, its susceptibility to corrosion in acidic environments is notable [4]. This vulnerability becomes particularly significant during industrial procedures such as acid descaling, oil well acidification, and acid pickling, which often involve handling mineral acids in elevated concentrations [5], leading to substantial damage to the carbon steel infrastructure.

Acidizing in petroleum oil wells is a critical technique for enhancing oil production, involving the injection of high-temperature acidic solutions into the wellbore to create channels in rock formations, allowing for improved oil and gas flow. This process also serves to dissolve debris within ageing wells, restoring and maximizing productivity. Various acids, including hydrofluoric acid (HF), acetic acid (CH_3COOH), chloroacetic acid ($ClCH_3COOH$), formic acid (HCOOH), and sulfamic acid (H_2NSO_3H), are utilized in acidizing treatments, with hydrochloric acid (HCl) being the most commonly employed acid, typically ranging from 5% to 28% concentration by weight. The acidizing method exposes the carbon steel pipelines of oil wells to a highly aggressive and corrosive environment [6].

Corrosion control in oil wells typically relies on four main methods: employing corrosion-resistant materials, implementing cathodic protection, applying coatings, and utilizing corrosion inhibitors. Among these approaches, corrosion inhibitors are particularly favoured for their practicality, cost-effectiveness, and efficiency in safeguarding oil wells against corrosion [7].

*Corresponding author: Prabin Kumar Mahato
Email: pkmahatoru@gmail.com
Paper received: 30.03.2025.
Paper accepted: 25.04.2025.

Inhibitors are added to the acid solution during the acidizing process to reduce the aggressive attack of the acid on oil wells. The effective acidizing inhibitors that are usually found in commercial formulations [1] are acetylenic alcohols [8], alkenylphenones[9], aromatic aldehydes[10], nitrogen-containing heterocyclics [11], and condensation products of carbonyls and amines[12]. Although effective at elevated concentrations, these inhibitors pose toxicity risks and are not environmentally friendly [13]. Consequently, the utilization of inorganic inhibitors is discouraged due to their detrimental impacts on human health and the environment [14]. In the 21st Century, the exploration of "green" or environmentally friendly corrosion inhibitors has become a focal point, aiming to deploy cost-effective molecules with minimal or zero environmental footprint. As of now, numerous alternative eco-friendly organic and inorganic inhibitors have been identified and explored [15, 16].

In the present study, the researchers aimed to investigate Myrrh Gum extract (MG) [17] as an eco-friendly corrosion inhibitor [18] which possesses several advantages such as low cost [19], environmental safety, and high inhibition efficiency [17].

2. EXPERIMENTAL

2.1. Material

The API 5CTP110 tubing served as the study's working electrode. Every sample intended for use in electrochemical tests was divided into squares of 3 x 3 x 1 cm. The supplier guaranteed the chemical composition of the steel under study, which included the following: C 0.24, Mn 1.37, Si 0.2, P 0.011, S 0.027, Cr 0.11, Ni 0.08, Mo 0.03, Al 0.01, Cu 0.1 and the remaining Fe. Every working electrode in contact with the electrolyte had a surface area of 2.85 cm^2. Before every examination, the surface was ready by a wet polishing process using silicon carbide abrasive sheets (grades 320 up to 800), followed by a distilled water rinse, and lastly with acetone degreasing.

2.2. Medium

Hydrochloric acid of analytical reagent grade 37% and distilled water were utilized to make the electrolyte solutions (0.5 mol/L).

2.3. Inhibitor

Myrrh Gum is a solid substance extracted from a small tree in the Commiphora genus. It is commonly used to produce perfumes, incense, and medicinal products due to its content of volatile oils, alcohol-soluble resins, and water-soluble gums. The primary natural components of Myrrh Gum are L-arabinose, 4-methyl D-glucuronic acid, and D-galactose acid, in a ratio of 1:3:4 [20].Glucuronic acid, which is one of its key constituents, contains a carboxyl group (-COOH)[21, 22]attached to the first carbon (C1) in its structure, a defining characteristic of uronic acids.The molecular structure of glucuronic acid is presented in Fig.1 [23].

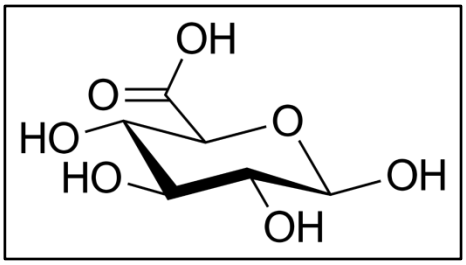

Figure 1. Molecular structure of Glucuronic aci

2.4. Electrochemical Techniques

Potentiodynamic polarization (PDP) and electrochemical impedance spectroscopy (EIS) were used to investigate the inhibitory impact of Myrrh for API 5CTP110 tubing in 0.5 mol/L M hydrochloric acid at 20°C. The Para Cell Electrochemical Cell Kit was used for all testing. It was made to accommodate a working, reference (Ag/AgCl), and counter (graphite) electrode. The working electrode and the graphite counter electrode were positioned in opposition to one another. The Gamry Instruments Potentiostat/Galvanostat/ZRA (Reference 3000) was linked to the electrochemical cell. The Gamry system incorporated specific software components, namely the GamryEchem Analyst software for data processing and the Gamry Instruments Framework for hardware control. All electrochemical assessments of the API 5CTP110 tubing were conducted in a 0.5 mol/L hydrochloric acid medium, both in the absence (blank) and presence of the inhibitor (Myrrh Gum), following a 30 minutesimmersion at 20°C. Tafel curves were generated by automatically varying the working electrode potential within the range of –0.25 to +0.25 V versus the open-circuit potential (OCP) at a scan rate of 0.5 mV/s. The anodic (*ba*) and cathodic (*bc*) Tafel slopes were extrapolated to determine the corrosion current (*Icorr*). The inhibition efficiency (η_{pol}) was computed using(Eq. 1):

$$\eta_{Pol}\% = \frac{I_{corr} - I_{corr(inh)}}{I_{corr}} \times 100 \quad (1)$$

Where *Icorr(inh)*and *Icorr* denote the corrosion current values in the presence and absence of the inhibitor, respectively. Electrochemical impedance

spectroscopy (EIS) experiments were executed under potentiostatic conditions spanning a frequency spectrum from 20 kHz to 50 mHz, with a 10mV peak-to-peak amplitude. The inhibition efficiency (η_{EIS}) was determined by contrasting the charge transfer resistance values in the presence (Rt) and absence ($\acute{R}t$) of Myrrh Gum, according to the following formula (Eq.2):

$$\eta_{EIS}\% = \frac{Rt - \acute{R}t}{Rt} \times 100 \qquad (2)$$

Surface Study by Scanning Electron Microscopy (SEM-EDX)

The surfaces of API 5CTP110 tubing specimens subjected to analysis included exposure to 0.5 mol/L hydrochloric acid both in the absence and presence of Myrrh Gum at 20°C. Utilizing the TESCANVEGA3 scanning electron microscope, we obtained images through scanning electron microscopy (SEM) and conducted energy-dispersive X-ray spectroscopic analysis (EDX).

3. RESULTS AND DISCUSSION

3.1. FT-IR spectroscopic analysis of MG

From Fig.2, a broad peak recorded at 3358cm^{-1} presented the stretching vibration of O–H (hydroxyl group). An absorption band around 2926 cm^{-1} was attributed to asymmetric and symmetric stretching vibrations of −CH2– groups (-CH group). In addition, the peak absorption recorded at 2103 cm^{-1} indicated the existence of stretching of carboxylic groups[24]. The peaks at 1732 cm^{-1} and 1633 cm^{-1} characterizes the C=O group and the C=C group respectively (which confirmed the presence of both ester and carboxyl groups). The peak located at 1424 cm^{-1} is attributed to −COO– symmetric stretching. The peak at 1370 cm^{-1} signifies the -CN group. Two peaks appeared 1235 cm^{-1} and 1017 cm^{-1} that are attributed to the vibration of the -CO group.

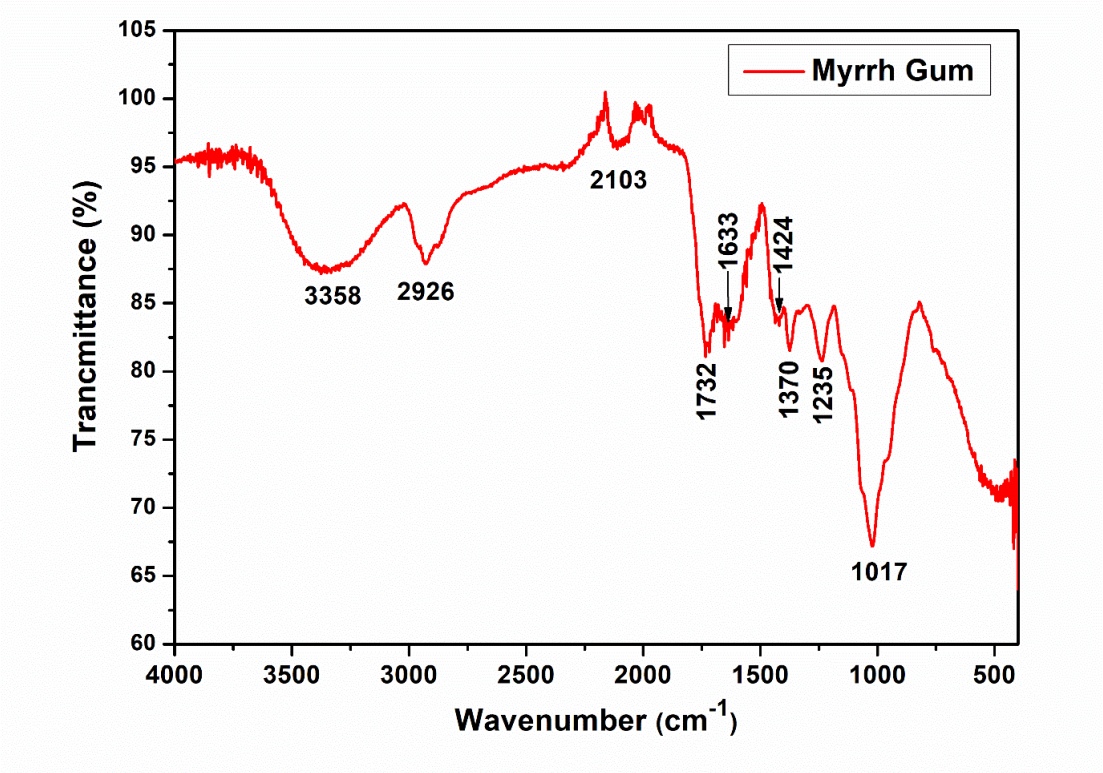

Figure 2. FTIR spectra of the Myrrh Gum (MG)

3.2. Inhibition effect of Myrrh Gum (MG)

Impedance measurements

Impedance tests were conducted to understand the properties and dynamics of the electrochemical reactions at the interface between API 5CTP110 tubing and HCl, both with and without MG. Fig.3shows the Nyquist, Bode modulus, and Bode phase diagrams from the EIS data gathered during the corrosion of API 5CTP110 tubing in a 0.5 M HCl solution, considering both scenarios where MG is absent and present in varying concentrations.

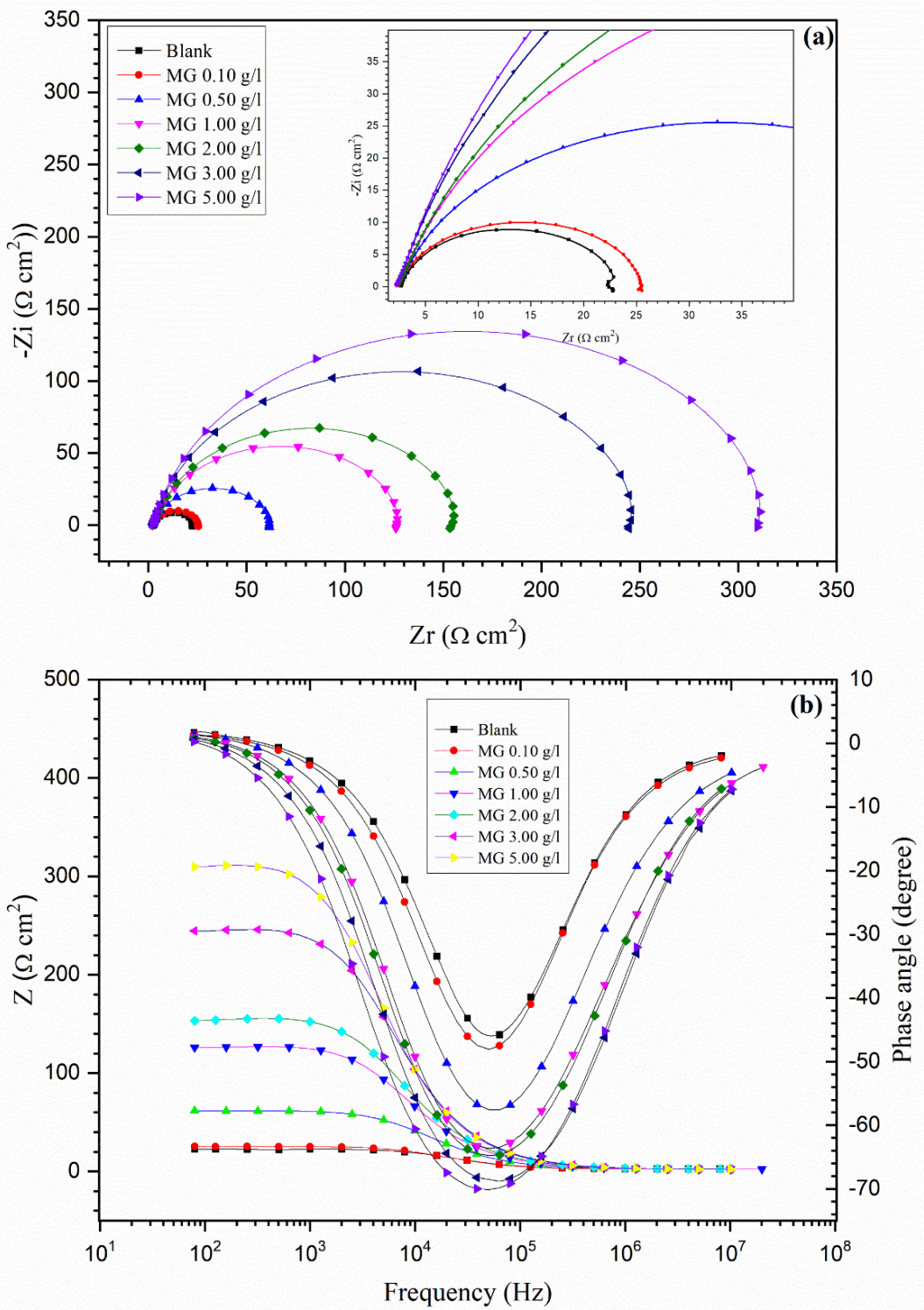

Figure 3. EIS plots for API 5CTP110 tubing in 0.5 M HCl medium without and with different concentrations of MG at 20°C, (a) Nyquist, (b) Bode modulus and Bode phase angle representations

The Nyquist plot (Fig.3.a) reveals depressed semicircles in both scenarios, with and without MG, indicating that the corrosion reactions are dominated by charge transfer processes [25, 26].Regardless of the presence of MG, all Nyquist plots maintain a similar configuration featuring a single capacitive loop, pointing to the geometric blocking effect as MG's mode of inhibition[27].An increase in the diameter of the Nyquist plots with rising MG concentrations shows MG's effectiveness in reducing the corrosion of API 5CTP110 tubing. However, careful estimation of

the Rt (charge transfer resistance) is necessary as the centers of these depressed semicircles are positioned below Zi = 0. The consistent shape of the Nyquist plots, whether MG is present or not, indicates that the inhibitor does not alter the dissolution mechanism of the steel but significantly affects the electrical properties of the double layer. Using the Impedance Model Editor from GamryEchem Analyst, an attempt was made to fit these results with an equivalent circuit model(Fig.4).The circuit consists of the solution resistance *Rs*, the constant phase element that represents the double-layer capacitance (CPE), and the charge transfer resistance *Rt*. The corresponding EIS data derived from this equivalent circuit model are displayed in Table1. Also, Fig.4 presents both the simulated and experimentally derived impedance curve for API 5CTP110 tubing immersed in 0.5 M hydrochloric acid solution with 3.00 g/L of MG.

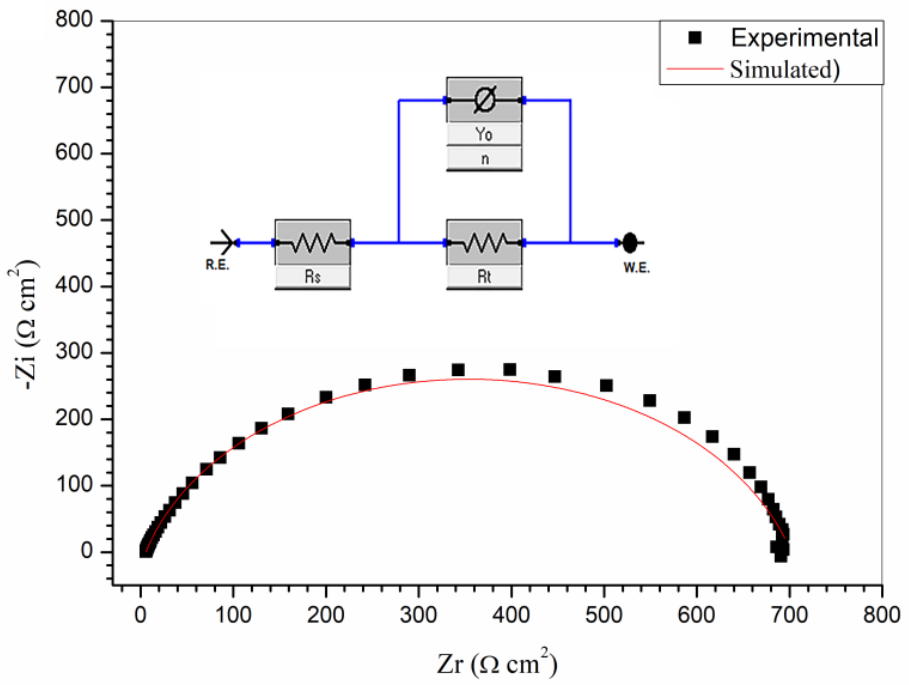

Figure 4. Nyquist plot of simulated data and experimental data, together with the equivalent circuit used to fit the impedance data, recorded for API 5CTP110 tubing in 0.5 M HCl containing 3 g/L MG

Table 1. EIS parameters for API 5CTP110 tubing in 0.5 M HCl without and with different concentrations of MG at 20°C

System/concentration	Rs, (Ω cm^2)	Y_0, (μΩ S^n cm^{-2})	n	Rt, (Ω cm^2)	Cdl, (μF cm^{-2})	η_{EIS}%
Blank	*2.7*	*686*	0.9*0*	*020.25*	423	-
0.10 g/L	*2.5*	*752*	0.88	*023.15*	421	*12*
0.50 g/L	*2.4*	*454*	0.8*7*	*060.54*	265	*66*
1.00 g/L	*2.2*	*342*	0.8*6*	*128.8*	204	*84*
2.00 g/L	*2.4*	*292*	0.8*7*	*157.5*	170	*87*
3.00 g/L	*2.2*	*214*	0.90	*250.1*	154	*92*
5.00 g/L	*2.2*	*225*	0.87	*317.8*	152	*93*

As the concentration of MG increased, there was a notable rise in the charge transfer resistance (*Rt*) of API 5CTP110 tubing. Specifically, the *Rt* value increased from 20.25Ωcm2 without MG to 250.1 Ω cm2 at a MG concentration of 3.00 g/L. It is important to note that at this concentration of 3.00 g/L, the Rt value reached a plateau and showed little further change. At a MG concentration of 3.00 g/L, the η_{EIS} exceeded 92%, demonstrating MG's efficacy as a corrosion inhibitor for API 5CTP110 tubing in an HCl solution. For more accurate fitting results, constant phase elements (CPE) were utilized in place of capacitors. The impedance of the CPE depends on the frequency, but its phase angle remains constant across frequencies (Eq.3)[28].

$$Z_{CPE} = Y_0^{-1}\left(j\omega\right)^{-n} \quad (3)$$

Here, Z_{CPE} denotes the impedance of a CPE, Y_0 is a scale factor indicative of the combined characteristics of the surface and electroactive species, independent of frequency, j represents the imaginary unit, ω is the angular frequency, and ω equals $2\pi f$, where f is the frequency. The parameter n represents a phase shift and relates to the slope of the log $|Z|$ versus log f curve, typically ranging from 0.5 to 1. Eq.4 was used to compute the double layer capacitance C_{dl}[29].

$$C_{dl} = Y_0 \left(2\pi f_{max}\right)^{n-1} \quad (4)$$

In this equation, f_{max} is the frequency at which the imaginary component of the impedance is at its maximum. Conversely, an increase in inhibition effectiveness is associated with a reduction in the metal's capacitance, as evidenced by the marked decrease in C_{dl} values from 423 μFcm^{-2} in the solution without MG to 152 μFcm^{-2} in the solution containing the highest MG concentration (3.00 g/L) at a temperature of 20°C.

3.3. Potentiodynamic polarization measurements

Fig.5 depicts the outcomes of potentiodynamic polarization tests conducted at 20°C on the surface of API 5CTP110 tubing in 0.5MHCl solutions, both with and without various concentrations of MG. The summarized results in Table2 include parameters such as corrosion current density, corrosion potential, anodic Tafel slope, and cathodicTafel slope, with the inhibition efficiency of MG calculated using Eq.1.Analysis of Fig.5 reveals a decrease in both cathodic and anodic current densities with increasing concentrations of MG, while the corrosion potential (*Ecorr*) remains unchanged, suggesting that MG acts as a mixed inhibitor[30].Further analysis of Fig.5 shows that the cathodic branches in both inhibited and uninhibited solutions of API 5CTP110 tubing display parallel Tafel lines, indicating that the corrosion reaction mechanism remains consistent and is governed by charge transfer processes, including hydrogen evolution and reduction of H^+ ions. However, the data in Table2 also shows a significant reduction in *Icorr* values as MG concentration increases, attributing to decreased hydrogen evolution and steel dissolution in the cathodic and anodic reactions, respectively, due to the inhibitor[31]. The effectiveness of an inhibitor in reducing corrosion can be influenced by two mechanisms: reducing the available reaction surface through geometric blocking and altering the activation energy of redox reactions. It is difficult to ascertain which mechanism predominates. If the geometric blocking effect is more significant, there would be no notable change in *Ecorr* after adding the inhibitor. The lack of substantial variation in *Ecorr* supports the dominance of the geometric blocking effect over activation energy changes[32].As the concentration of MG increases, the efficacy of the inhibitor peaks at 91% at 3.00 g/L, as shown in Table 2, demonstrating a strong correlation between the data from EIS and potentiodynamic polarization tests.

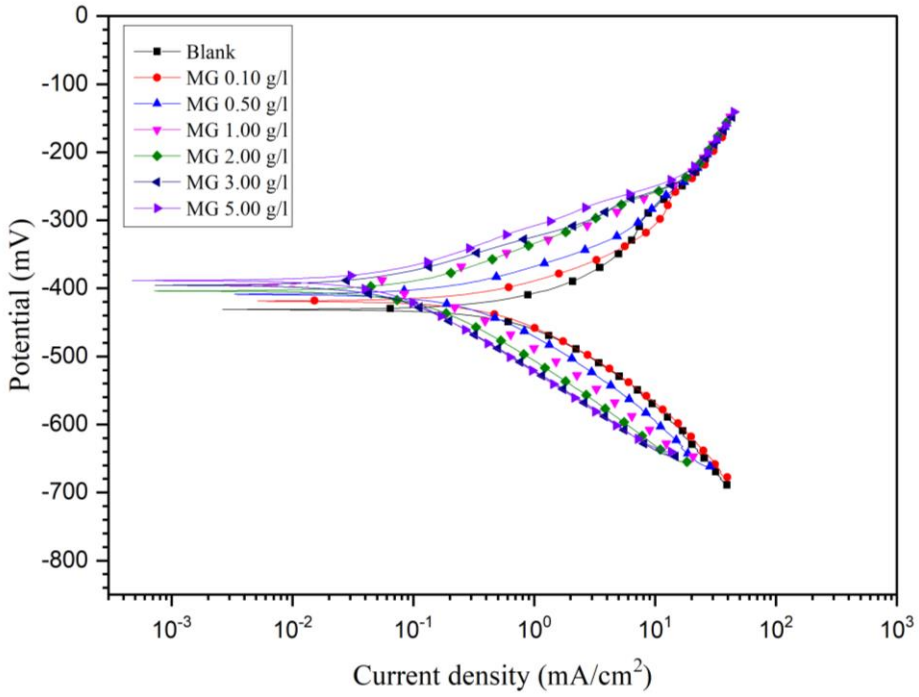

Figure 5. Potentiodynamic polarization curves for API 5CTP110 tubing in 0.5 M HCl without and with different concentrations of MG at 20°C

Table 2. Potentiodynamic polarization parameters for API 5CTP110 tubing in 0.5 M HCl without and with different concentrations of MG at 20°C

System/ Concentration	Ecorr, (mV)	Icorr, (μA)	- *bc,* (mV dec^{-1})	Ba,(mV dec^{-1})	η_{pol}, %
Blank	*-426*	*948*	14*2*	*101*	-
0.10 g/L	*-419*	*844*	14*1*	*99*	*11*
0.50 g/L	-4*07*	*367*	*127*	*75*	*61*
1.00 g/L	-*390*	190	129	70	*80*
2.00 g/L	-400	144	124	75	84
3.00 g/L	-396	87	116	64	91
5.00 g/L	-389	71	116	68	92

3.4. Adsorption isotherm and standard free energy of adsorption

The present study assessed various adsorption isotherms and identified the Langmuir adsorption isotherm as the most appropriate model to describe the adsorption behaviour of the investigated inhibitor, as depicted in Fig.6. This isotherm establishes a relationship between the surface coverage ($\theta = \eta_{EIS}\%/100$) and the inhibitor concentration (C) in the electrolyte[33].

$$\frac{C}{\theta} = \frac{1}{K_{ads}} + C \qquad (5)$$

The adsorption process is characterized by the adsorption constant K_{ads}, which can be derived from the linear plots of C/θ against C, yielding slopes close to unity. Additionally, the standard free energy of adsorption ΔG°_{ads} is calculated using K_{ads} through Eq.6[33, 34].

$$\Delta G^{\circ}_{ads} = -RT\ ln(1\times 10^{6} K_{ads}) \qquad (6)$$

where 1 x 10^6 represents the concentration of water molecules in mg/L, R is the universal gas constant, and T is the absolute temperature. The values of ΔG_{ads} and K_{ads} are presented in Table3. The value of K_{ads} serves as an indicator of the strength of the adsorption forces between the inhibitor molecules and the metal surface [28].

In general, if the ΔG°_{ads} value is up to -20 kJ/mol, it indicates physical adsorption between charged molecules and a charged metal due to electrostatic interaction. On the other hand, if the ΔG°_{ads} value is below -40 kJ/mol, it shows chemisorption, which involves charge sharing or transfers from the inhibitor to the metal surface to form a coordinate bond [35].In this investigation, the value of ΔG°_{ads} is 9.99 kJ/mol demonstrating that the adsorption of MG on API 5CTP110 tubing surface includes physical adsorption. This conclusion is supported by similar findings from the study of Ebenso et all. [36].

Table 3. Langmuir adsorption isotherm parameters for API 5CTP110 tubing in 0.5 M HCl solution containing MG at 20°C

Isotherm mode	Linear correlation coefficient	Slope	K_{ads} (L/g)	ΔG°_{ads} (kJmol^{-1})
Langmuir	0.99673	0.98592	2.7993	-19.67

3.5. Surface analysis by SEM-EDX

Fig.6 presents microscope images and corresponding chemical analysis for the polished metal surfaces, both with and without the inhibitor (MG), to demonstrate the effectiveness of MG as confirmed by EIS and polarization curve methods. When the pipeline steel was immersed in 0.5 M HCl, a corrosion product formed on its surface, as shown in Fig.6.a, due to the ongoing corrosion process. In contrast, the microscopy image of the specimen treated with the inhibitor (Fig.7.b) shows no visible corrosion product.

To identify the surface components of API 5CTP110 tubing after 72 hours of exposure to 0.5 M HCl, Energy Dispersive X-ray Spectroscopy (EDX) analysis was performed (Table4). In the absence of the inhibitor, the EDX spectra revealed prominent peaks for oxygen and chloride elements. However, for the API 5CTP110tubing exposed to 0.5 M HCl containing 3 g/L of MG, the spectra indicated a reduction in the oxygen and chloride ratios, likely due to the adsorption of MG on the tubing surface.

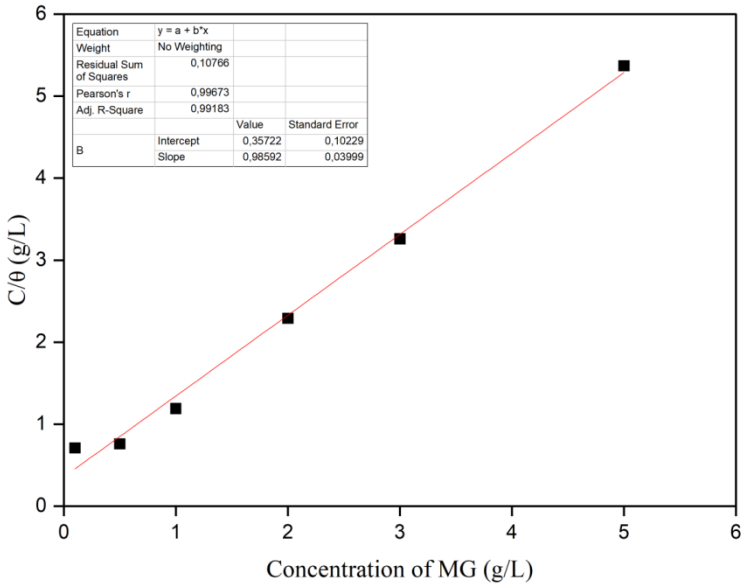

Figure 6. Langmuir isotherm adsorption mode of MG on the API 5CTP110 tubing in 0.5 M HCl at 20°C (from EIS measurements).

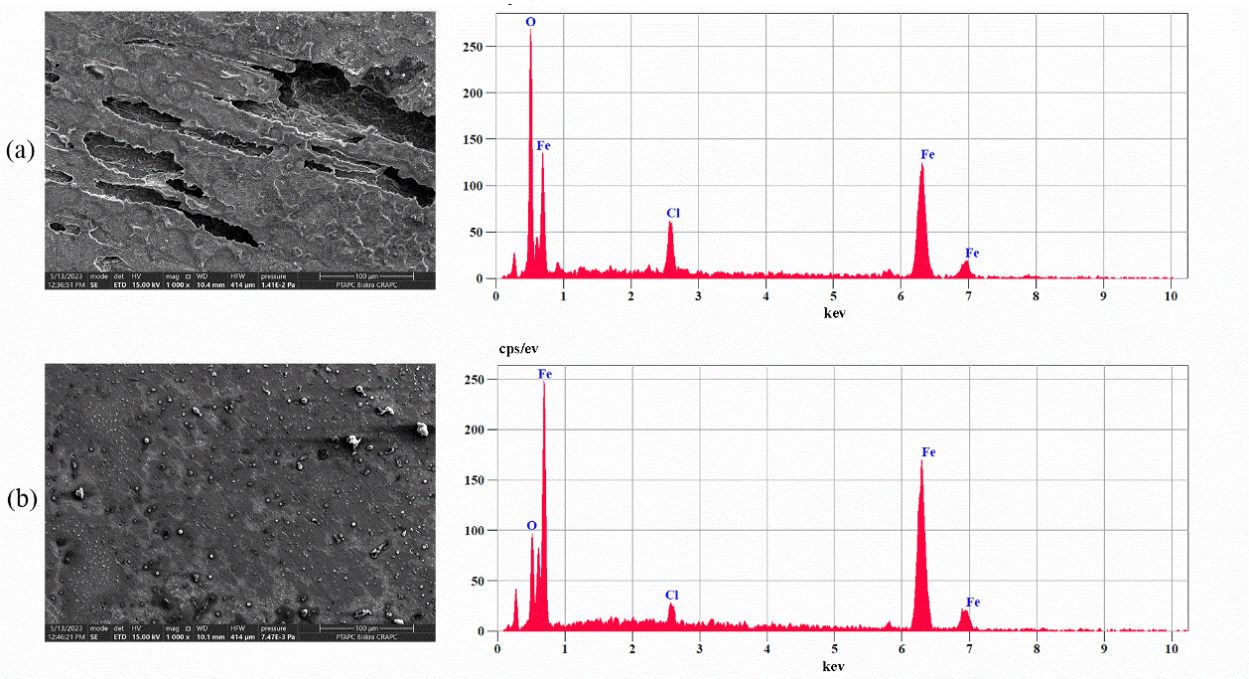

Figure 7. SEM images of API 5CTP110 tubing in 0.5 M HCl at 20°C before and after 72 h immersion: (a) in 0.5 M HCl without and (b) in 0.5 M HCl with 2 g/L MG

Table 4. Content of elements obtained from EDX spectra for API 5CTP110 tubing

Element	Weight %	
	Steel + 0.5 M HCl	Steel + 0.5 M HCl + 3 g/L GM
Iron	77.17	90.78
Oxygen	16.14	6.41
Chlorine	6.69	2.81

3.6. Mechanism of Corrosion Inhibition

Dominant component of MG is polysaccharides with a carboxyl functional group (glucuronic acid)[20]. The free energy of adsorption of MG is –19.67 kJ mol/L, which indicates that the adsorption mechanism of the MG on API 5CTP110 steel surface is a physical absorption. Glucuronic acid molecules can be adsorbed on the steel surface via

electrostatic interaction between the protonated glucuronic acid molecules and the charged metal surface. The API 5CTP110 steel surface has a positive charge in the hydrochloric acid[37], so due to the electrostatic repulsion, the protonated glucuronic acid molecules cannot get close to the steel surface. Since the anions of Cl^- could be specifically adsorbed on the API 5CTP110 steel surface, the latter becomes negatively charged and therefore increases the tendency of adsorption of the protonated glucuronic acid chains on API 5CTP110 steel surface by electrostatic interaction (physisorption).

4. CONCLUSIONS

This study on the corrosion inhibition properties of Myrrh Gum (MG) for API 5CTP110 tubing in hydrochloric acid (HCl) solution yielded the following key findings:

MG is an effective inhibitor for API 5CTP110 tubing in 0.5 M HCl, with inhibition efficiency increasing with concentration and reaching a maximum of 92% at 3 g/L.

The adsorption behaviour of MG on the tubing surface aligns with the Langmuir adsorption isotherm.

The calculated ΔG°_{ads} value confirms that the adsorption of MG on the steel surface occurs predominantly through physical adsorption mechanisms.

Potentiostatic polarization data indicate that MG functions as a mixed-type inhibitor, affecting both anodic and cathodic reactions.

Electrochemical impedance spectroscopy (EIS) and polarization studies suggest that the inhibition mechanism of MG primarily involves a geometric blocking effect, reducing the active surface area exposed to the corrosive medium.

5. REFERENCES

[1] K. Haruna, I. Obot, N. Ankah, A. Sorour, T. Saleh (2018) Gelatin: A green corrosion inhibitor for carbon steel in oil well acidizing environment, J. Mol. Liq., 264, 515-525. DOI: 10.1016/j.molliq.2018.05.058.

[2] W. Zhang, H.-J. Li, M. Wang, L.-J. Wang, F. Shang, Y.-C. Wu (2018) Halogen-substituted acridines as highly effective corrosion inhibitors for mild steel in acid medium, J. Phys. Chem. C, 122, 25349-25364. DOI: 10.1021/acs.jpcc.8b07015.

[3] A.H. Alamri (2020) Localized corrosion and mitigation approach of steel materials used in oil and gas pipelines – An overview, Eng. Fail. Anal., 116, 104735. DOI: https://doi.org/10.1016/j.engfailanal.2020.104735.

[4] M.A.M. El-Haddad, A. Bahgat Radwan, M.H. Sliem, W.M.I. Hassan, A.M. Abdullah (2019) Highly efficient eco-friendly corrosion inhibitor for mild steel in 5 M HCl at elevated temperatures: experimental & molecular dynamics study, Sci. Rep., 9, 3695. DOI: 10.1038/s41598-019-40149-w.

[5] M. Goyal, S. Kumar, I. Bahadur, C. Verma, E.E. Ebenso (2018) Organic corrosion inhibitors for industrial cleaning of ferrous and non-ferrous metals in acidic solutions: A review, J. Mol. Liq., 256, 565-573. DOI: https://doi.org/10.1016/j.molliq.2018.02.045.

[6] A. Singh M.A. Quraishi (2015) Acidizing corrosion inhibitors: a review, J. Mater. Environ. Sci, 6, 224-235.

[7] D. Dwivedi, K. Lepková, T. Becker (2017) Carbon steel corrosion: a review of key surface properties and characterization methods, RSC Adv., 7, 4580-4610. DOI: https://doi.org/10.1039/C6RA25094G

[8] A. Frignani, C. Monticelli, F. Zucchi, G. Trabanelli (2014) Acetylenic alcohols as inhibitors of iron acid corrosion. Improvement of the inhibition efficiency of a class of substances based on their action mechanism, Int. J. Corros. Scale Inhib, 3, 105. DOI: 10.17675/2305-6894-2014-3-2-105-119.

[9] M. Salman, K. Ansari, V. Srivastava, D.S. Chauhan, J. Haque, M. Quraishi (2021) Chromeno naphthyridines based heterocyclic compounds as novel acidizing corrosion inhibitors: Experimental, surface and computational study, J. Mol. Liq., 322, 114825. DOI: https://doi.org/10.1016/j.molliq.2020.114825.

[10] M. Galai, M.E. Touhami, M. Oubaaqa, K. Dahmani, M. Ouakki, M. Khattabi, Z. Benzekri, R. lachhab, S. Kaya, N. Bulut, S. Briche, S. Boukhris (2023) Electrochemical, Characterization, and Quantum Chemical Studies of Two Newly Synthesized Aromatic Aldehydes-Based Xanthene Diones as Corrosion Inhibitors for Mild Steel in 1 M Hydrochloric Acid, J. Bio- Tribo-Corros., 9, 63. DOI: 10.1007/s40735-023-00778-1.

[11] J. Wang, L. An, J. Wang, J. Gu, J. Sun, X. Wang (2023) Frontiers and advances in N-heterocycle compounds as corrosion inhibitors in acid medium: Recent advances, Adv. Colloid Interface Sci., 103031. DOI: https://doi.org/10.1016/j.cis.2023.103031.

[12] M. Yadav, S. Kumar, P. Yadav (2013) Corrosion Inhibition of Tubing Steel during Acidization of Oil and Gas Wells, J. Pet. Eng., 2013. DOI: 10.1155/2013/354630.

[13] D. Singh A. Dey (1993) Synergistic effects of inorganic and organic cations on inhibitive performance of propargyl alcohol on steel dissolution in boiling hydrochloric acid solution, Corrosion, 49, 594-600. DOI: https://doi.org/10.5006/1.3316090.

[14] F.G. Liu, M. Du, J. Zhang, M. Qiu (2009) Electrochemical behavior of Q235 steel in saltwater saturated with carbon dioxide based on new imidazoline derivative inhibitor, Corros. Sci., 51, 102-109. doi: https://doi.org/10.1016/j.corsci.2008.09.036.

[15] X. Li, S. Deng, H. Fu, G. Mu (2010) Synergistic inhibition effect of rare earth cerium(IV) ion and sodium oleate on the corrosion of cold rolled steel in phosphoric acid solution, Corros. Sci., 52, 1167-1178. DOI: https://doi.org/10.1016/j.corsci.2009.12.017.

[16] X. Li, S. Deng, H. Fu, G. Mu (2009) Synergistic inhibition effect of rare earth cerium(IV) ion and 3,4-dihydroxybenzaldehye on the corrosion of cold rolled steel in H2SO4 solution, Corros. Sci., 51, 2639-2651. DOI: https://doi.org/10.1016/j.corsci.2009.06.047.

[17] S.Y. Al-Nami A.E.-A.S. Fouda (2020) Corrosion Inhibition Effect and Adsorption Activities of methanolic myrrh extract for Cu in 2 M HNO3, Int. J. Electrochem. Sci., 15, 1187-1205. doi: https://doi.org/10.20964/2020.02.23.

[18] B. Tan, B. Xiang, S. Zhang, Y. Qiang, L. Xu, S. Chen, J. He (2021) Papaya leaves extract as a novel eco-friendly corrosion inhibitor for Cu in H2SO4 medium, J. Colloid Interface Sci., 582, 918-931. doi: https://doi.org/10.1016/j.jcis.2020.08.093.

[19] N. Hossain, M. Asaduzzaman Chowdhury, M. Kchaou (2021) An overview of green corrosion inhibitors for sustainable and environment friendly industrial development, J. Adhes. Sci. Technol., 35, 673-690. DOI: 10.1080/01694243.2020.1816793.

[20] M. Rinaudo (2014) Biomateriales basados en un polisacárido natural: el alginato, TIP Revista Especializada en Ciencias Químico-Biológicas, 17, 92-96.

[21] H. Hu, J. Li, W. Jiang, Y. Jiang, Y. Wan, Y. Wang, F. Xin, W. Zhang (2024) Strategies for the biological synthesis of D-glucuronic acid and its derivatives, World J. Microbiol. Biotechnol., 40, 94. DOI: 10.1007/s11274-024-03900-8.

[22] A. Wadouachi J. Kovensky (2011) Synthesis of Glycosides of Glucuronic, Galacturonic and Mannuronic Acids: An Overview, Molecules, 16, 3933-3968. doi: 10.3390/molecules16053933.

[23] A. Richel, F. Nicks, P. Laurent, B. Wathelet, J.-P. Wathelet, M. Paquot (2012) Efficient microwave-promoted synthesis of glucuronic and galacturonic acid derivatives using sulfuric acid impregnated on silica, Green Chemistry Letters and Reviews, 5, 179-186. doi: 10.1080/17518253.2011.607852.

[24] C.-S. Wu (2009) Renewable resource-based composites of recycled natural fibers and maleated polylactide bioplastic: Characterization and biodegradability, Polym. Degrad. Stab., 94, 1076-1084. https://doi.org/10.1016/j.polymdegradstab.2009.04.002.

[25] A. Singh, K.R. Ansari, D.S. Chauhan, M.A. Quraishi, H. Lgaz, I.-M. Chung (2020) Comprehensive investigation of steel corrosion inhibition at macro/micro level by ecofriendly green corrosion inhibitor in 15% HCl medium, J. Colloid Interface Sci., 560, 225-236. doi: https://doi.org/10.1016/j.jcis.2019.10.040.

[26] M. Djellab, H. Bentrah, A. Chala, H. Taoui, S. Kherief, B. Bouamra (2020) Synergistic effect of iodide ions and bark resin of Schinus molle for the corrosion inhibition of API5L X70 pipeline steel in H2SO4, Mater. Corros., 71, 1276-1288. DOI: https://doi.org/10.1002/maco.202011533.

[27] D. Wang, Y. Li, B. Chen, L. Zhang (2020) Novel surfactants as green corrosion inhibitors for mild steel in 15% HCl: Experimental and theoretical studies, Chem. Eng. J., 402, 126219. doi: https://doi.org/10.1016/j.cej.2020.126219.

[28] S.A. Umoren (2016) Polypropylene glycol: A novel corrosion inhibitor for ×60 pipeline steel in 15% HCl solution, J. Mol. Liq., 219, 946-958. DOI: https://doi.org/10.1016/j.molliq.2016.03.077.

[29] M. Djellab, H. Bentrah, A. Chala, H. Taoui (2019) Synergistic effect of halide ions and gum arabic for the corrosion inhibition of API5L X70 pipeline steel in H2SO4, Mater. Corros., 70, 149-160. doi: https://doi.org/10.1002/maco.201810203.

[30] R. Solmaz, G. Kardaş, M. Çulha, B. Yazıcı, M. Erbil (2008) Investigation of adsorption and inhibitive effect of 2-mercaptothiazoline on corrosion of mild steel in hydrochloric acid media, Electrochim. Acta, 53, 5941-5952. doi: https://doi.org/10.1016/j.electacta.2008.03.055.

[31] I.B. Obot, A. Meroufel, I.B. Onyeachu, A. Alenazi, A.A. Sorour (2019) Corrosion inhibitors for acid cleaning of desalination heat exchangers: Progress, challenges and future perspectives, J. Mol. Liq., 296, 111760. doi: https://doi.org/10.1016/j.molliq.2019.111760.

[32] H. Taoui, H. Bentrah, A. Chala, M. Djellab (2019) Bark resin of Schinus molle as an eco-friendly inhibitor for API 5L X70 pipeline steel in HCl medium, Mater. Corros., 70, 511-520. doi: https://doi.org/10.1002/maco.201810477.

[33] O. Sotelo-Mazon, S. Valdez, J. Porcayo-Calderon, M. Casales-Diaz, J. Henao, G. Salinas-Solano, J.L. Valenzuela-Lagarda, L. Martinez-Gomez (2019) Corrosion protection of 1018 carbon steel using an avocado oil-based inhibitor, Green Chemistry Letters and Reviews, 12, 255-270. DOI: 10.1080/17518253.2019.1629698.

[34] M.M. Solomon, S.A. Umoren, A.U. Israel, I.G. Etim (2016) Synergistic inhibition of aluminium corrosion in H2SO4 solution by polypropylene glycol in the presence of iodide ions, Pigment Resin Technol., 45, 280-293. doi: 10.1108/PRT-01-2015-0010.

[35] H. Bentrah, Y. Rahali, A. Chala (2014) Gum Arabic as an eco-friendly inhibitor for API 5L X42 pipeline steel in HCl medium, Corros. Sci., 82, 426-431. DOI: https://doi.org/10.1016/j.corsci.2013.12.018.

[36] E. Ebenso, N. Eddy, A. Odiongenyi (2009) Corrosion Inhibition and Adsorption Properties of Methocarbamol on Mild Steel in Acidic Medium, Port. Electrochim. Acta, 27, 13-22. DOI: 10.4152/pea.200901013.

[37] S. Kherief, M. Djellab, H. Bentrah, A. Chala, B. Bouamra, H. Taoui (2023) Corrosion Inhibition Efficiency of Ghars Date Extract on API 5L X70 Pipeline Steel in Hydrochloric Acid, Protection of Metals and Physical Chemistry of Surfaces, 59, 1306-1314. doi: 10.1134/S2070205123701162.

IZVOD

EFIKASNOST INHIBITORA KOROZIJE GUME MIRTE NA CEVIMA API 5CTP110 U HLOROVODONIČNOJ KISELINI

Ispitivana su svojstva inhibicije korozije gume mirte (MG) na cevima API 5CTP110 u rastvoru HCl od 0,5 M. Studija je pokazala da MG pokazuje izuzetne inhibitorne performanse, postižući efikasnost od 92% pri optimalnoj koncentraciji od 3 g/L. Analiza je otkrila da adsorpcija molekula MG na površinu čelika prati model Langmirove izoterme, što ukazuje na proces kojim dominira fizička adsorpcija. Pored toga, MG deluje kao inhibitor mešovitog tipa, efikasno ublažavajući i anodne i katodne reakcije. Ovi nalazi ističu potencijal gume mirte kao isplativog i ekološki prihvatljivog inhibitora korozije za industrijske primene, posebno u kiselim sredinama. Upotreba MG je u skladu sa održivim praksama, pružajući održivu alternativu tradicionalnim sintetičkim inhibitorima i doprinoseći razvoju zelenih strategija za sprečavanje korozije.
Ključne reči: *Ekološki inhibitor korozije, API 5CTP110 cevi, guma mirte, hlorovodonična kiselina, EIS*

Naučni rad
Rad primljen: 30.03.2025.
Rad prihvacen: 25.04.2025.